

ORIGINAL  
RESEARCH

Y. Kawai  
M. Sumi  
T. Nakamura

# Turbo Short $\tau$ Inversion Recovery Imaging for Metastatic Node Screening in Patients with Head and Neck Cancer

**BACKGROUND AND PURPOSE:** A rapid and sensitive MR imaging technique would be beneficial for screening of metastatic nodes in the neck. We preliminarily evaluated the coronal MR imaging with a turbo short  $\tau$  inversion recovery (STIR) sequence for that purpose.

**METHODS:** The coronal turbo STIR imaging (repetition time [TR]/echo time [TE]/inversion time [TI] = 3850 ms/20 or 80 ms/180 ms) and axial fat-suppressed spectral presaturation with inversion recovery (SPIR) T2-weighted imaging (fsT2WI) (TR/TE = 3500 ms/80 ms) were performed on 29 patients with head and neck cancer. We obtained coronal turbo STIR images and axial fsT2WI of the necks. The section thickness, intersection gap, matrix size, and field of view were the same in both techniques. The diagnostic ability for metastatic nodes was assessed at each neck level by using various cutoff size criteria. The nodal involvement was confirmed by histologic examination.

**RESULTS:** The image acquisition time for the whole neck by coronal turbo STIR and axial fsT2WI techniques was approximately 2 minutes and 4 minutes, respectively. When the size criteria (cutoff sizes of short axis diameter were 8 mm at level I and 5 mm at levels II and III) were used, the STIR imaging yielded compromised diagnostic ability having 100% sensitivity and 100% negative predictive value (NPV). fsT2WI technique yielded 100% sensitivity and 100% NPV by using cutoff sizes of 6 mm at levels I and II and 5 mm at level III.

**CONCLUSION:** Coronal STIR imaging provided a rapid screening technique for cervical metastatic nodes and could be a diagnostic tool before detailed MR studies of the neck.

The presence of lymph node metastasis in the neck is an important prognostic determinant in staging cancers and planning radiation therapy for patients with head and neck cancer.<sup>1</sup> Van den Brekel et al<sup>2</sup> refined the previously reported size criteria for detecting metastatic cervical nodes by cross-sectional techniques. The performance of MR imaging in diagnosing metastatic nodes in the neck was not highly ranked.<sup>3,4</sup> Thereafter, several attempts have been made to evaluate various MR imaging techniques for discriminating metastatic nodes from benign lesions.<sup>5</sup>

A recent report described the first successful application of high-resolution MR imaging in discriminating metastatic nodes from benign nodes in the necks of patients with head and neck cancer.<sup>6</sup> The high-resolution MR imaging techniques provided information about the changes in nodal architectures that were characteristic of metastatic nodes (eg, central nodal necrosis and obliteration of fat tissue in the hilum). The precise diagnosis of the metastatic nodes in the neck could be achieved by the high-resolution MR imaging by using a small-sized surface coil. However, the detailed imaging of the whole neck requires extended image acquisition time and, as a result, patient movement may hamper the image quality. Therefore, the rapid and sensitive imaging technique would be very beneficial for the diagnosis of metastatic nodes in the neck. Additional detailed MR examinations could be more efficient after such a screening of the neck.

Some investigators have discussed the utility of short  $\tau$  in-

version recovery (STIR) MR imaging for the detection of metastatic nodes in various cancers.<sup>7-9</sup> A recent report showed that the STIR imaging for the detection of metastasis in mediastinal and hilar nodes in patients with non-small-cell lung cancer yielded 93% sensitivity and 87% specificity on a per-patient basis.<sup>10</sup> Furthermore, the diffusion-weighted imaging with single-shot, STIR-echo-planar technology has been successfully applied to whole-body imaging. This high-contrast imaging technology is not degraded too much by motion artifact.<sup>11</sup>

Therefore, the aim of this study was to evaluate the STIR MR imaging as a screening tool for the metastatic nodes in the necks of patients with head and neck cancer. In this study, we sought to determine whether the coronal turbo STIR technique is appropriate for the rapid and sensitive MR screening of metastatic nodes in the neck. We reasoned that a short image acquisition time (less than 3 minutes) without the need for whole-neck image reconstruction is mandatory for establishing an appropriate turbo STIR screening technique.

## Materials and Methods

### Patients

We performed a hypothesis-driven study on 29 consecutive patients (6 women and 23 men; average age, 60  $\pm$  15 years; age range, 28–81 years) with head and neck squamous cell carcinoma, who had received STIR and fsT2WI MR imaging examinations and underwent surgical excision of the primary tumors and neck dissection at our hospital from 2002 to 2004. The primary sites of the carcinomas in these patients included the tongue (8 patients), oropharynx (8 patients), nasopharynx (3 patients), larynx (2 patients), buccal mucosa (2 patients), upper gingiva (1 patient), palate (1 patient), parotid gland (1 patient), and an unknown site (1 patient). We staged the

Received July 29, 2005; accepted after revision October 31.

From the Department of Radiology and Cancer Biology, Nagasaki University School of Dentistry, Nagasaki, Japan.

Address correspondence to Dr. Takashi Nakamura, Department of Radiology and Cancer Biology, Nagasaki University School of Dentistry, 1-7-1 Sakamoto, Nagasaki 852-8588, Japan.

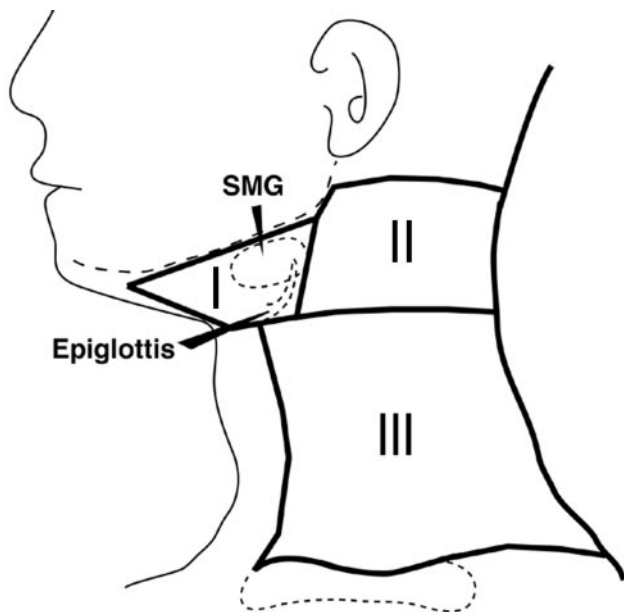


**Fig 1.** Schematic drawing of classification of cervical lymph nodes into 3 neck levels (I–III). Details are explained in the “Materials and Methods” section. SMG, submandibular gland.

tumors according to the TMN clinical classification based on MR imaging findings.<sup>12</sup>

### Classification of the Nodes

On coronal turbo STIR images, some of the neck levels (for example, levels III and IV, as classified by Curtin et al,<sup>3</sup> and IA and IB, IIA and IIB, and III to V, as classified by Som et al<sup>13</sup>) were not readily differentiated. Therefore, we categorized cervical nodes into 3 levels (levels I, II, and III) (Fig 1). In brief, the nodes at level I were those located in the submental and submandibular region, including the area anterior to the posterior margin of the submandibular gland. The nodes at level II were those in the area whose anterior border coincided with the posterior boundary of level I. All the nodes in the jugular and spinal accessory chain above the epiglottis were included in this group. The nodes at level III included those in the remaining part of the neck situated above the clavicle.

### Surgical Correlation and Histologic Examination

All patients underwent either unilateral or bilateral radical dissection of the neck. The surgeon mapped the excised nodes relative to the surrounding structures of the neck. The nodes were then processed for histologic examinations. A pathologist classified the nodes that were histologically positive or negative for metastasis according to the neck levels (I–III), and determined whether a positive node was present at each level of the neck. The presence of tumor in any node indicated that the corresponding neck level was positive for metastasis. The histologic results were then compared with those obtained by turbo STIR MR imaging, and the decision was made in consensus by 2 radiologists. In patients who underwent unilateral radical dissection of the neck, the follow-up included periodic examination of the contralateral necks by sonography or MR imaging, or both, for nodal metastasis. These “clinically silent” necks were not irradiated and followed by “watch and wait” approach. Therefore, we categorized these necks as those with clinically silent nodes. As a result, we studied 58 unilateral necks and 174 neck levels in 29 patients.

### MR Imaging

The necks of patients with head and neck cancer were studied with a 1.5T superconductive MR unit (Gyrosan Intera 1.5T Master; Philips Medical Systems, Best, The Netherlands) by using a head and neck coil (Synergy Head/Neck Coil) or a 20-cm surface coil (Flex L coil). Turbo STIR imaging (repetition time [TR]/echo time [TE]/inversion time [TI]/number of signal intensity acquisition [NSA] = 3850 ms/20 or 80 ms/180 ms/1 or 2) was performed to obtain coronal MR images of the necks. To compensate for the image intensity inhomogeneity that is inherent to the use of surface coils, the CLEAR (Constant Level Appearance) postprocessing technique (Philips Medical Systems) was used to improve visualization of tissues that are located beyond the coil’s diameter. The echo-train length (turbo factor) ranged from 5 to 16, depending on the TEs. The fsT2WI imaging (TR/TE/NSA = 3500 ms/80 ms/2) was performed to obtain axial images of the neck. For both techniques (STIR and fsT2WI), the section thickness was 4 mm, and the intersection gap was 0.8 mm. The MR imaging was performed with a matrix of 192 × 128 and a field of view of 23 cm. We also used reversed STIR images, which resemble images in scintigraphy or in positron-emission tomography (PET) and is familiar to clinicians.

### Interpretation of MR Images

On the basis of sequential, coronal turbo STIR images and axial fsT2WI images obtained from each patient, we identified nodes as discrete, round, or oval areas of moderate to high signal intensity in the neck. Some of these nodes were palpable, but the others were nonpalpable. On coronal images, the nodes were steadily differentiated from other organs in the neck, such as the blood vessels and muscles. Two radiologists determined separately the short-axis diameter of the nodes without knowledge of histologic findings. The short-axis diameter is defined as a minimal axis diameter on the largest area of a node. Therefore, the short and long axes cross at right angles on the area of a node. We used “short axis diameter” of the nodes because this size criterion was shown to be better for metastatic nodes than maximum axial diameter.<sup>14</sup>

On direct coronal turbo STIR images and axial fsT2WI images, we calculated separately the sensitivity (true-positive results/[true-positive results + false-negative results]) and specificity (true-negative results/[true-negative results + false-positive results]) by using various size criteria (cutoff sizes of short axis diameter).

Negative predictive values (NPVs) and positive predictive values were also used to assess the performance of the MR imaging criteria (various cutoff sizes of short axis diameter or the presence or absence of hyperintense areas in the nodes) in the detection of metastatic nodes. The negative predictive value is the percentage of neck levels interpreted by using the MR imaging criteria as neck levels negative for metastasis that were negative for metastasis on histologic examination. The positive predictive value is the percentage of neck levels interpreted as positive for metastasis that were histopathologically proved to be metastasized.

### Results

We found that turbo STIR imaging with different TEs resulted in similar results (Fig 2). The coronal turbo STIR imaging required approximately 2 minutes and the fsT2WI (spectral presaturation with inversion recovery [SPIR]) required approximately 4 minutes for the whole-neck imaging. On turbo STIR images, a node was characteristically depicted as a discrete, round, or ovoid area of intermediate to high signal intensity (Figs 3A–5A). Extremely hyperintense areas in such

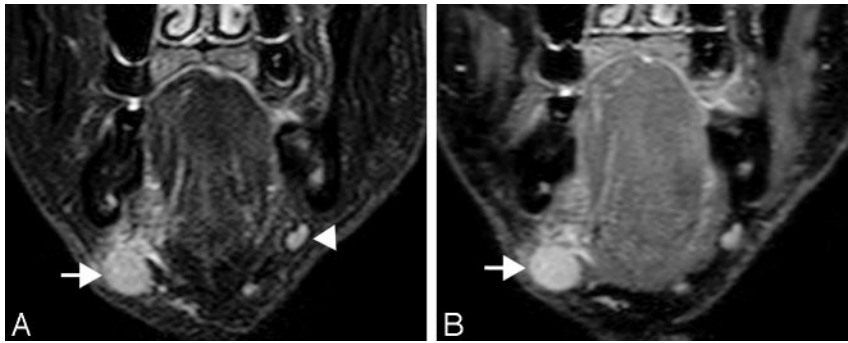


**Fig 2.** A 74-year-old man with oral floor cancer. Comparison of turbo STIR images obtained by different TEs. A, Coronal turbo STIR image (TR/TE/TI/NSA/turbo factor = 3850 ms/80 ms/180 ms/2/16) shows metastatic node (arrow) at level I. Benign node is noted on ipsilateral side at same neck level (arrowhead).

B, Coronal turbo STIR image (TR/TE/TI/NSA/turbo factor = 3850 ms/20 ms/180 ms/1/5) shows same metastatic node (arrow) as in A. Similar results were obtained by using these techniques.

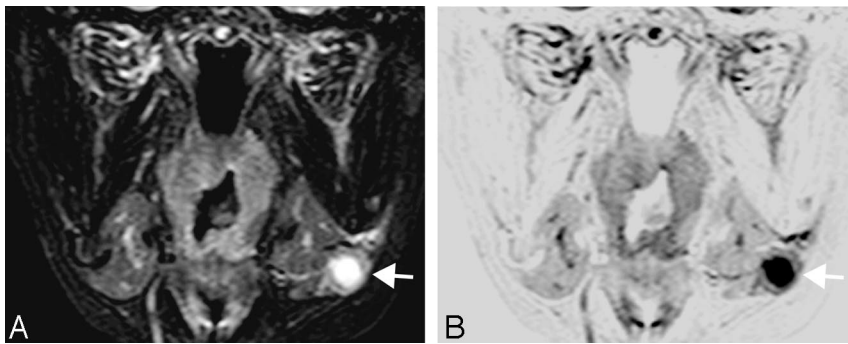


**Fig 3.** A 64-year-old woman with tongue cancer. A, Coronal turbo STIR image (TR/TE/TI/NSA/turbo factor = 3850 ms/80 ms/180 ms/2/16) shows metastatic node (arrow) at neck level I. The metastatic node is 10 mm in short axis diameter and contains high-intensity necrotic area.

B, Reversed coronal turbo STIR image of A.

nodes were very suggestive of the presence of nodal necrosis existing in cancer nests. Therefore, the possible criteria for differentiating metastatic nodes from benign nodes might be their sizes and hyperintense signals suggestive of nodal necrosis. The muscles displayed signals with an intermediate intensity. The subcutaneous tissues, fatty marrow, and cortical bone displayed low intensity signals. We also used reversed STIR images, in which the nodes displayed low to intermediate intensity, and nodal necrosis displayed extremely low signal intensity (Figs 3B–5B); these reversed images resemble scintigraphy and PET and are familiar to clinicians.

Histologic examinations revealed that of 174 neck levels, 48 neck levels were positive for metastatic nodes; of these, 8, 25, and 15 neck levels were positive for metastasis at levels I, II, and III, respectively. When the smaller size criteria (5 or 6 mm in short axis diameter) were used, the turbo STIR imaging yielded 100% sensitivity at the expense of specificity. On the other hand, using the larger size criteria resulted in low sensitivity and high specificity (Tables 1 and 2). We reasoned that intending the turbo STIR sequence as a screening technique, compromised criteria with a high sensitivity and intermediate specificity should be achieved. Therefore, we concluded that the best cutoff points were 8 mm for nodes located at level I and 5 mm for nodes at levels II and III (Tables 1 and 2). These size criteria yielded 100% sensitivity and 100% NPV at levels I to III. On the other hand, the best cutoff points were 6 mm at levels I and II, and 5 mm at level III by the fST2WI technique; these criteria provided 100% sensitivity and 100% NPV (Tables 1 and 3).

When a node was diagnosed as metastatic because of area(s) of very high intensity suggestive of nodal necrosis, the STIR imaging yielded very low sensitivity (13%–36%) and 100% specificity. We found that necrosis occurred only in nodes having a short axis diameter  $\geq 10$  mm. Therefore, metastatic nodes smaller than 10 mm in short axis diameter were diagnosed as positive by tumor invasion per se.

**Table 1: Imaging diagnosis of metastasis-positive and -negative necks by direct coronal turbo STIR imaging or axial fat-suppressed T2-weighted (SPIR) imaging**

Size* (mm)	Meta	Level of Neck (n)					
		I (58):		II (58):		III (58):	
		meta (+) (8), meta (-) (50)		meta (+) (25), meta (-) (33)		meta (+) (15), meta (-) (43)	
$\geq 5$	+	32	36	47	46	25	22
	-	26	22	11	12	33	36
$\geq 6$	+	24	26	44	44	23	19
	-	34	32	14	14	35	39
$\geq 7$	+	15	18	44	41	18	17
	-	43	40	14	17	40	41
$\geq 8$	+	14	13	36	35	17	17
	-	44	45	22	23	41	41
$\geq 9$	+	9	9	31	26	11	13
	-	49	49	27	32	47	45
$\geq 10$	+	6	5	29	24	8	12
	-	52	53	29	34	50	46

**Note:**—STIR indicates short  $\tau$  inversion recovery; meta, metastasis.  
\*Cutoff point of short-axis diameter.

### Discussion

In this preliminary report, we have proposed turbo STIR imaging as a candidate for a rapid, sensitive MR imaging technique for the screening of metastatic nodes in the neck of patients with head and neck cancer. We found that, at each level of the neck, if the nodes were judged based only on the size determined by coronal turbo STIR images, high sensitivity (100%) and moderate specificity (64% to 88%) were achieved. The criteria about the presence or absence of nodal necrosis, which is considered pathognomonic of nodal metastasis from head and neck squamous cell carcinomas determined by CT, sonography, and MR imaging,<sup>15</sup> provided high specificity (100%). On the other hand, the sensitivity was very low at any level of the neck (13% to 36%). We reasoned that the diagnosis-

**Table 2: Diagnostic ability of direct coronal turbo STIR imaging for detecting metastatic nodes in the neck**

Criteria for Metastatic Node	Level of Neck*		
	I	II	III
Size cutoff point (mm)			
≥5	100/52/25/100	<b>100/33/53/100</b>	<b>100/77/60/100</b>
≥6	100/68/33/100	96/39/55/93	93/79/61/97
≥7	100/86/53/100	96/39/55/93	80/86/67/93
≥8	<b>100/88/57/100</b>	96/64/67/95	80/88/70/93
≥9	88/96/78/98	92/76/74/93	73/100/100/91
≥10	63/98/83/94	92/82/79/93	53/100/100/86

**Note:**—STIR indicates short  $\tau$  inversion recovery; PPV, positive predictive value; NPV, negative predictive value.

\*Values are expressed as percentages as follows: sensitivity/specificity/PPV/NPV. Bold data indicate compromised diagnostic ability at each level.

**Table 3: Diagnostic ability of axial SPIR imaging for detecting metastatic nodes in the neck**

Criteria for Metastatic Node	Level of Neck*		
	I	II	III
Size cutoff point (mm)			
≥5	100/44/22/100	100/36/54/100	<b>100/84/68/100</b>
≥6	<b>100/64/31/100</b>	<b>100/42/57/100</b>	87/86/68/95
≥7	88/78/39/98	96/48/59/94	87/90/76/95
≥8	88/88/54/98	92/64/66/91	87/91/76/95
≥9	88/96/78/98	80/82/77/84	80/98/92/93
≥10	63/100/100/94	80/88/83/85	80/100/100/93

**Note:**—SPIR indicates axial fat-suppressed T2-weighted; PPV, positive predictive value; NPV, negative predictive value.

\*Values are expressed as percentages as follows: sensitivity/specificity/PPV/NPV. Bold data indicate compromised diagnostic ability at each level.

tic ability with high sensitivity is needed for the clinically feasible screening technique. Taken together, we concluded that the size criteria are suitable for the present purpose.

The coronal turbo STIR screening technique should be performed on all patients with head and neck cancer before the following detailed MR examinations that use, for example, a small-sized surface coil. We preferred the coronal turbo STIR sequence with a TE of 80 ms, because this sequence reduced the background signals, such as those from the muscles, more effectively than the sequence with a shorter TE (Fig 2).

We also analyzed diagnostic ability by axial fsT2WI in detecting neck levels with metastatic nodes and compared the results with those by direct coronal turbo STIR imaging (Tables 1–3). We found that the 2 techniques provided comparable abilities in detecting metastatic neck levels in patients with head and neck cancer. However, compared with the 2 techniques, faster image acquisition time and relative refractoriness to susceptibility artifacts are advantages of the coronal turbo STIR technique as a screening tool for the detection of metastatic nodes.

Most pathologic tissues are proton-rich and have prolonged T1 relaxation and T2 decay times, resulting in high signal intensity on STIR images. The previous report showed that the STIR technique is highly sensitive for the detection of pathologic lesions but is not specific for malignancy.<sup>16</sup> Therefore, this MR technique cannot be used to differentiate benign nodes from malignant nodes, when the obtained imaged data are interpreted based only on the signal intensity of pathologic lesions. However, if the sizes of the nodes are also evaluated, the STIR technique could be applicable as a screening technique for metastatic nodes in the neck. This notion was based

on the previous findings that size criteria were effective in differentiating benign nodes from metastatic nodes during CT and sonographic examinations.<sup>17–19</sup> The best cutoff points for metastatic nodes were found to vary at different levels of the neck.<sup>20</sup> In rough accordance with these preceding results, we found that the best cutoff points for metastatic nodes were greater at the levels I and II compared with that at level III (Tables 2 and 3).

The present findings that the use of size criteria is essential in differentiating benign and malignant nodes in the neck were consistent with those in a preceding study using an STIR MR imaging sequence, where the authors appraised a short-axis diameter greater than 10 mm as a criterion for abnormal nodes in children.<sup>16</sup> The higher cutoff point (10 mm) was used in the preceding study, perhaps because its cutoff point was for lymphomas but not for metastatic nodes. In this context, nodal lymphomas were reported to be relatively larger than metastatic nodes in the neck.<sup>21</sup> We found that nodal necrosis occurred only in large nodes ( $\geq 10$  mm), indicating that metastatic nodes smaller than 10 mm were positive by tumor invasion per se. These findings were consistent with the previous studies using sonography and CT, where the size criteria alone provided good diagnostic abilities in differentiating benign and metastatic nodes in the neck.<sup>19,20</sup>

The coronal turbo STIR imaging allows whole neck imaging within a short image acquisition time, is refractory to susceptible artifacts compared with axial fsT2WI, and can yield high sensitivity comparable with the fsT2WI technique. Therefore, this technique may be applicable to clinical practice as a screening tool for the detection of metastatic nodes in patients with head and neck cancer. However, an evaluation relative to nuclear medicine studies by using fluorine-18 fluorodeoxyglucose PET needs additional extensive studies using large cohorts.

Takahara et al<sup>11</sup> recently proposed a new MR technique designated as diffusion-weighted, whole-body imaging with background body signal intensity suppression (DWIBS), whereby the background body signals from the vessels, muscles, and fat were effectively suppressed by the diffusion-weighted and/or the STIR pulse. Indeed, we observed phase-ghosting artifacts on direct coronal STIR images of the necks (Figs 4 and 5). Therefore, the DWIBS technique may be a promising technology for diagnosing a wider range of nodal diseases, including lymphomas as well as metastatic nodes.

Compared with high-resolution MR imaging with a small-sized surface coil, the coronal turbo STIR imaging is not suitable for the assessment of internal architectures of the nodes. In particular, smaller nodes ( $< 6$  mm in short-axis diameter) may frequently be missed by the turbo STIR technique. A recent study using a microscopy coil showed that MR criteria on nodal architectures yielded 86% sensitivity and 94% specificity for discriminating metastatic nodes in the neck.<sup>6</sup> Another shortcoming of the coronal turbo STIR imaging is that body background signals from the blood vessels were not suppressed; therefore, it may be difficult to distinguish the vessels and lymph nodes. One of the advantages of the proposed coronal turbo STIR imaging, however, is that the technique allows concomitant visualization of the primary lesions.



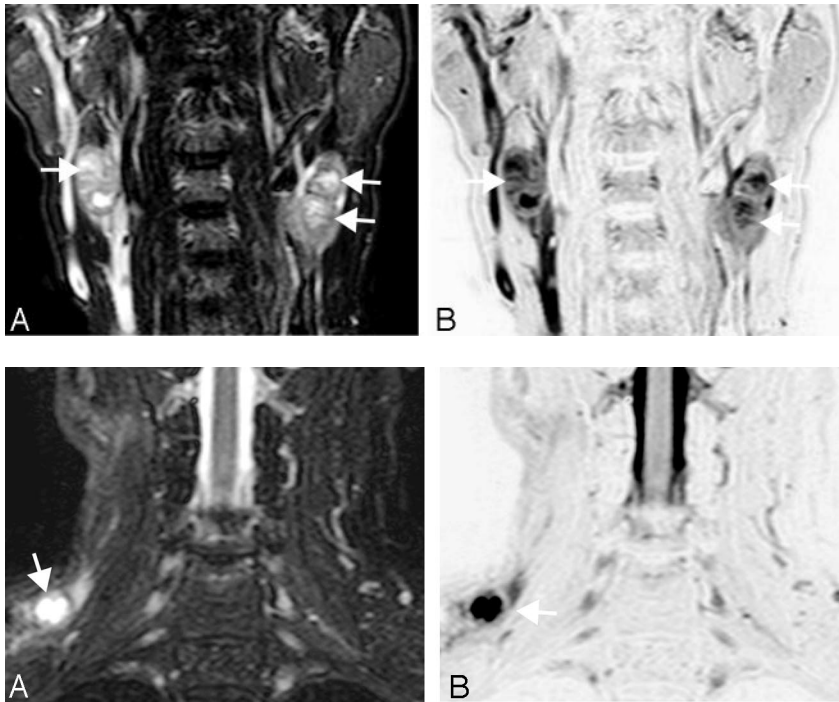


**Fig 4.** A 56-year-old man with nasopharyngeal cancer. *A*, Coronal turbo STIR image (TR/TE/TI/NSA/turbo factor = 3850 ms/80 ms/180 ms/2/16) shows 3 metastatic nodes with necrotic foci at level II (arrows). Two metastatic nodes (12 mm [top] and 14 mm [bottom]) are on the left side of the neck, and 1 node (17 mm) on the right side. *B*, Reversed coronal turbo STIR image of *A*.

**Fig 5.** A 71-year-old man with laryngeal cancer. *A*, Coronal turbo STIR image (TR/TE/TI/NSA/turbo factor = 3850 ms/80 ms/180 ms/2/16) shows a metastatic node (11 mm) with central nodal necrosis at neck level III (arrow). *B*, Reversed coronal turbo STIR image of *A*.

## Conclusion

Coronal turbo STIR imaging is a rapid and sensitive MR technique for detecting metastatic nodes in the neck. We propose this technique as a screening tool before high-resolution MR imaging using a small-sized surface coil for the diagnosis of metastatic nodes in the necks of patients with head and neck cancer.

## References

- Anzai Y, Brunberg JA, Lufkin RB. **Imaging of nodal metastases in head and neck.** *J Magn Reson* 1997;7:774–83
- van den Brekel MWM, Castelijns JA, Snow GB. **The size of lymph nodes in the neck on sonograms as a radiologic criterion for metastasis: How reliable is it?** *AJNR Am J Neuroradiol* 1998;19:695–700
- Curtin HD, Ischwaran H, Mancuso AA, et al. **Comparison of CT and MR imaging in staging of neck metastases.** *Radiology* 1998;207:123–30
- Yang WT, Lam WW, Yu MY, et al. **Comparison of dynamic helical CT and dynamic MR imaging in the evaluation of pelvic nodes in cervical carcinoma.** *AJR Am J Roentgenol* 2000;175:759–66
- Fishbein NJ, Noworolski SM, Henry RG, et al. **Assessment of metastatic cervical adenopathy using dynamic contrast-enhanced MR imaging.** *AJNR Am J Neuroradiol* 2003;24:301–11
- Sumi M, Van Cauteren M, Nakamura T. **MR microimaging of benign and malignant nodes in the neck.** *AJR Am J Roentgenol* 2006;186:749–57.
- Walker R, Kessar P, Blanchard R, et al. **Turbo STIR magnetic resonance imaging as a whole-body screening tool for metastases in patients with breast carcinoma: preliminary clinical experience.** *J Magn Reson Imaging* 2000;11:343–50
- Eustace S, Tello R, DeCarvalho V, et al. **Whole body turbo STIR MRI in unknown primary tumor detection.** *J Magn Reson Imaging* 1998;8:751–53
- Takenaka D, Ohno Y, Hatabu H, et al. **Differentiation of metastatic versus non-metastatic mediastinal lymph nodes in patients with non-small cell lung cancer using respiratory-triggered short inversion time inversion recovery (STIR) turbo spin-echo MR imaging.** *Eur J Radiol* 2002;44:216–24
- Ohno Y, Hatabu H, Takenaka D, et al. **Metastases in mediastinal and hilar lymph nodes in patients with non-small cell lung cancer: quantitative and qualitative assessment with turbo STIR spin-echo MR imaging.** *Radiology* 2004;231:872–79
- Takahara T, Imai Y, Yamashita T, et al. **Diffusion weighted whole body imaging with background body signal suppression (DWIBS): technical improvement using free breathing, STIR and high resolution 3D display.** *Radiat Med* 2004;22:275–82
- Sobin LH, Wittekind C, eds. *TNM Classification of Malignant Tumors*, 6th ed. International Union against Cancer. New York: Wiley-Liss; 2002
- Som PM, Curtin HD, Mancuso AA. **Imaging-based nodal classification for evaluation of neck metastatic adenopathy.** *AJR Am J Roentgenol* 2000;174:837–44
- van den Brekel MWM, Stel HV, Castelijns JA, et al. **Cervical lymph node metastasis: assessment of radiologic criteria.** *Radiology* 1990;177:379–84
- King AD, Tse GMK, Yuen EHY, et al. **Necrosis in metastatic neck nodes: diagnostic accuracy of CT, MR imaging, and US.** *Radiology* 2004;230:720–26
- Kellenberger CJ, Epelman M, Miller SF, et al. **Fast STIR whole-body MR imaging in children.** *Radiographics* 2004;24:1317–30
- Ariji Y, Kimura Y, Hayashi N, et al. **Power Doppler sonography of cervical lymph nodes in patients with head and neck cancer.** *AJNR Am J Neuroradiology* 1998;19:303–07
- Sumi M, Ohki M, Nakamura T. **Comparison of sonography and CT for differentiating benign from malignant cervical lymph nodes in patients with head and neck squamous cell carcinomas.** *AJR Am J Roentgenol* 2001;176:1019–24
- Eida S, Sumi M, Yonetsu K, et al. **Combination of helical CT and Doppler sonography in the follow-up of patients with clinical N0 stage neck disease and oral cancer.** *AJNR Am J Neuroradiol* 2003;24:312–18
- Yonetsu K, Sumi M, Izumi M, et al. **Contributions of blood flow information to the precision of metastatic cervical nodes in patients with head and neck cancer: assessment in relation to anatomical levels of the neck.** *AJNR Am J Neuroradiol* 2001;22:163–69
- Sumi M, Sakihama N, Sumi T, et al. **Discrimination of metastatic cervical lymph nodes with diffusion-weighted MR imaging in head and neck cancer.** *AJNR Am J Neuroradiol* 2003;24:1627–34